Anti-Sway Position Control of an Automated Transfer Crane Based on Neural Network Predictive PID Controller

Jin-Ho Suh, Jin-Woo Lee
Department of Electrical Engineering, Dong-A National University, 840, Hadan-dong, Saha-gu, Busan 604-714, Korea
Young-Jin Lee
Department of Electrical Instrument and Control, Korea Aviation Polytechnic College, 438 Egeum-dong, Sachon City, Kyungnam 664-180, Korea
Kwon-Soon Lee*
Division of Electrical, Electronic, and Computer Engineering, Dong-A University, 840, Hadan-dong, Saha-gu, Busan 604-714, Korea

In this paper, we develop an anti-sway control in proposed techniques for an ATC system. The developed algorithm is to build the optimal path of container motion and to calculate an anti-collision path for collision avoidance in its movement to the finial coordinate. Moreover, in order to show the effectiveness in this research, we compared NNP PID controller to be tuning parameters of controller using NN with 2 DOF PID controller. The simulation and experimental results show that the proposed control scheme guarantees performances, trolley position, sway angle and settling time in NNP PID controller than other controller. As the results in this paper, the application of NNP PID controller is analyzed to have robustness about disturbance which is wind of fixed pattern in the yard. Accordingly, the proposed algorithm in this study can be readily used for industrial applications.

Key Words : Automated Transfer Crane (ATC), Neural Network Predictive (NNP) Control, Predictive Control, NN Auto Tuner, Anti-Sway Control, Collision Avoidance Path

1. Introduction

During 1996, The Center of Transport Technology (CTT) has initiated the FAMAS (First, All Modes, All sizes) program. The goal of the program is to develop a new generation of container terminals capable to handle all modalities of transshipment of all container sizes with an equal service level. This concerns all modalities, including the coming Jumbo Container Vessel with a capacity of eight to ten thousand TEU (Twenty-foot Equivalent Unit). Moreover the increase of quantity of goods transport has also expected Super Post-Panamax Vessel to appear and the growth of international container transport has also led to increase demands for quay and terminal capacity in ports all over the world. To execute this program a consortium has been formed by several major, transport related companies like ECT, Siemens Nederland, Nelcon and The Delft University of Technology (Klaassens et al., 1999).

To accomplish the goal of the program, a highly automated terminal has to be developed. Although, robotizing is not the main goal of the program, it is the opinion that handling containers

* Corresponding Author,
E-mail : kslee@dau.ac.kr
TEL : +82-51-200-6950; **FAX** : +82-51-200-7743
Department of Electrical Engineering, Dong-A National University, 840, Hadan-dong, Saha-gu, Busan 604-714, Korea. (Manuscript **Received** April 6, 2004; **Revised** November 29, 2004)

with a throughput of 500,000 TEU a year or more can only be done economically and efficiently by robotizing stacking and terminal transport. The program is subdivided into several projects, where New Terminal Control (NewCon), Jumbo Container Crane (JCC) and Automated Guided Vehicles (AGV) are the most important projects. New technologies will be developed or enhanced like anti-sway controllers, stacking algorithms, AGV control and terminal information techniques. Moreover the researches for new automatic container terminal in many countries make effort to reduce costs of port transportation. That is, the demands made on container handling in international seaports are continuously increasing, because both the capacity of the vessels is increasing, and the service time of container vessels should be decreasing. In order to minimize this service time a new generation of the so-called Jumbo Container Cranes will be developed.

In the last decade, we have seen an increase in complexity of the technical systems, especially in the introduction of semi-automated systems. Rotterdam's ECT terminal has been leading in this respect with the introduction of an AGV and an ASC at the former Delta-Sealand Terminal in 1992. An automated transfer crane (ATC) control system is required with highest productivity. This tendency may also show the optimal way to solve the employment problems, the cost saving problems and the improvement of efficiency in port systems (Sakawa and Shindo, 1982).

To consider nonlinear elements of an ATC, we are to design a controller for crane automatic position and anti-sway. In these points, PID controller has been widely used in actual industry because of its convenience and ordinary usage for user. As transfer crane has lots of dynamic characteristics, PID parameters must be changed in varying conditions automatically. Therefore this paper presents a control system for this generation of an ATC using neural network (NN) which is one of robust intelligent control theory about nonlinearity. Especially, the proposed predictive control system in this paper is composed of three components ; i) neural network predictor (NNP), ii) PID controller and iii) NN auto tuner. Moreover we should present an ATC system with anti-sway control expressed by three techniques above and construct the proposed controller in online manner. The simulation and experimental results are shown that the developed controller for an ATC system has better driving performances and anti-sway than a conventional PID controller.

2. Modeling of an Automated Transfer Crane

2.1 Generalized coordinates of an ATC

In this paper, we assume that the considered overhead crane system is satisfied with the following conditions :

(1) A transfer crane supposes that do only plane moment, that is, the sway of container supposes that happen in plane made by transfer direction and container of trolley.

(2) Elastic deformation of a transfer crane construction is very small value.

(3) Attenuate influence that is happened in frictional resistance or drive mechanism is microscopic.

(4) The container has hanged down in rope that there is no mass.

Figure 1 shows the coordinate systems of a overhead crane and its load. In Fig. 1, XYZ is

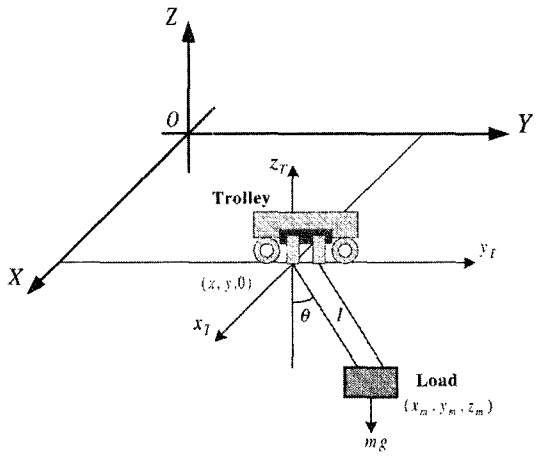

Fig. 1 Coordinate systems of an overhead crane

the fixed coordinate system and $x_T y_T z_T$ is the trolley coordinate system which moves with the trolley. The origin of the trolley coordinate system is $(x, y, 0)$ in the fixed coordinate system. Each axis of the trolley coordinate system is parallel to the counterpart of the fixed coordinate system. θ is the swing angle of the load in an arbitrary direction in space and has two components, i.e., $\theta=(\theta_x, \theta_y)^T$, where θ_x is the swing angle projected on the $x_T z_T$ plane and θ_y is the swing angle measured from the $x_T z_T$ plane.

The position of the load (x_m, y_m, z_m) in the fixed coordinate system is given by

$$x_m=x+l\sin\theta_x\cos\theta_y \tag{1}$$

$$y_m=y+l\sin\theta_y \tag{2}$$

$$z_m=-l\cos\theta_x\cos\theta_y \tag{3}$$

where l is the rope length. The purpose of this research is to control the motion of both crane and its load.

Hence x, y, l, and θ are defined as the generalized coordinates to describe the motion.

2.2 Dynamic equation of an ATC system

In this section, Lee (1997; 1998) reported results that the equations of motion of an overhead crane system are derived using Lagrange's equation (Furuta, 1980). Especially, in this research, the load is considered as a point mass, and the mass and stiffness of the rope are also neglected.

The kinetic energy of the overhead crane and its load K and the potential energy of the load P are given as follows:

$$K=\frac{1}{2}(M_x\dot{x}^2+M_y\dot{y}^2+M_l\dot{l}^2)+\frac{1}{2}mv_m^2 \tag{4}$$

$$P=mgl(1-\cos\theta_x\cos\theta_y) \tag{5}$$

where M_x, M_y, and M_l are the x (traveling), y (traversing), and l (hoisting) components of the transfer crane mass and the equivalent masses of the rotating parts such as motors and their drive trains, respectively. m is the load mass, g is the gravitational acceleration, and v_m denotes the load speed defined by:

$$\begin{aligned}v_m^2&=\dot{x}_m^2+\dot{y}_m^2+\dot{z}_m^2\\&=\dot{x}^2+\dot{y}^2+\dot{l}^2+l^2\dot{\theta}_x^2\cos^2\theta_y+l^2\dot{\theta}_y^2\\&\quad+2(\dot{l}\sin\theta_x\cos\theta_y+l\dot{\theta}_x\cos\theta_x\cos\theta_y\\&\quad-l\dot{\theta}_y\sin\theta_x\sin\theta_y)\dot{x}\\&\quad+2(\dot{l}\sin\theta_y+l\dot{\theta}_y\cos\theta_y)\dot{y}\end{aligned} \tag{6}$$

Also, Rayleigh's dissipation function is described as follows:

$$D=\frac{1}{2}(D_x\dot{x}^2+D_y\dot{y}^2+D_l\dot{l}^2) \tag{7}$$

where D_x, D_y, and D_l denote the viscous damping coefficients associated with the x, y, and l motions, respectively. Then, the equation of motion of a transfer crane system are obtained by Lagrange's equations associated with the generalized coordinate, $q=(x, y, l, \theta_x, \theta_y)_T$.

For small swing, $\sin\theta_x\approx\theta_x$, $\sin\theta_y\approx\theta_y$, $\cos\theta_x\approx1$, and $\cos\theta_y\approx1$. In this case, the high order terms in the nonlinear model can be neglected with the trigonometric functions approximated. Then the nonlinear model for an ATC system is simplified to be the linearized model as follows:

$$(M_x+m)\ddot{x}+ml\ddot{\theta}_x+D_x\dot{x}=f_x \tag{8}$$

$$(M_y+m)\ddot{y}+ml\ddot{\theta}_y+D_y\dot{y}=f_y \tag{9}$$

$$(M_l+m)\ddot{l}+D_l\dot{l}-mg=f_l \tag{10}$$

$$l\ddot{\theta}_x+\ddot{x}+g\theta_x=0 \tag{11}$$

$$l\ddot{\theta}_y+\ddot{y}+g\theta_y=0 \tag{12}$$

where f_x, f_y, and f_l are the driving forces for the x, y, and l motions, respectively. In practice, the maximum acceleration of an overhead crane is much smaller than the gravitational acceleration, and the rope length l is kept constant or slowly varying while the cranes are in motion. In this crane system, the object to be controlled is the trolley position, the wire lope length, and the load swing angle. Also, this linearized dynamic model consists of the travel dynamics Eqs. (8) and (11), the traverse dynamics Eqs. (9) and (12), and the independent load hosting dynamics Eq. (10). The travel and traverse dynamics are decoupled and symmetric, which means that the control of a three-dimensional overhead crane is transformed into that of two independent two-dimensional

transfer cranes having the same load hoisting dynamics.

3. Path Planning Method of an ATC System

3.1 Problem statement of path planning for an ATC system

In case that an ATC system transport containers in yard, it can be distributed into 5 actuation varieties as shown in Fig. 2. In this figure, the section AB exists an only perpendicular motion of hoist to B point and has the maximum perpendicular velocity, the section BC increases maximally when the velocity of trolley is 0. The other hand, the velocity of hoist decreases maximum to minimum. Also, a swing angle of an ATC system may be 0 at the point C as possible as one can. The swing angle in the section CD exists small and the maximum horizontal moving of trolley exists only. Finally, the section DC and EF have the reverse action between the section AB and BC, respectively.

In this paper, we shall propose the optimal path moving method in order to solving the path moving problem of trolley in an ATC system. Therefore the technique development for investigating the moving paths is required to many researches in order to improve work ability of an ATC system and prevent a loading container from collision in yard. To assign the optimal path for container moving in this research, we propose an effective search algorithm for collision avoidance path which connect both the incoming position A of containers and the outgoing position F and develop the tracking of assigned collision avoidance path and the predictive moving algorithm for transporting containers in the minimum time simultaneously (Sohn et al., 2003a ; 2003b).

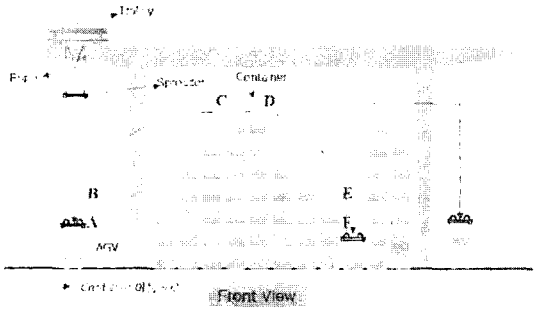

Fig. 2 Each transportation path of an ATC

3.2 A path search and minimum distance calculation for moving an ATC

In this paper, the containers are divided into lattice format of a rectangular parallelepiped as size and configuration of theirs, and each unit-lattice is composed by the characteristic coordinates (X_i, Y_i) as shown in Fig. 3. Then we will execute the modeling in free space with respect to apply the concept of configuration space based on the distributive map of containers, and then calculate an anti-collision path to be not occurred during the moving motion of container to apply the optimal best-first search method for searching the optimal path. Therefore the anti-

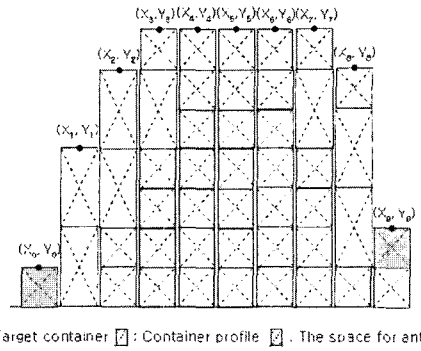

Fig. 3 An imaginary transportation path and an ATC profile

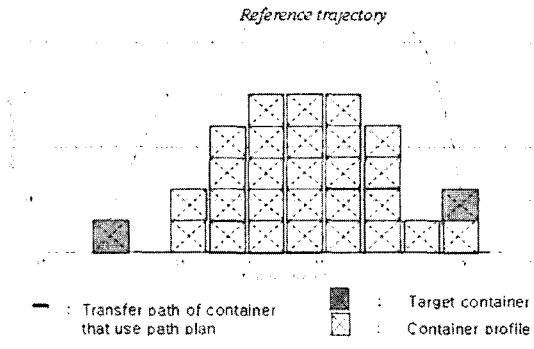

Fig. 4 The path search of reference trajectory for an ATC profile

collision path expresses the knot point located in the conveyance path of container, and then each cross point also represents the reference point of unit-lattice as shown in Fig. 4.

To apply a yard map concept, the method for searching the path, which does not happen to collision between a carried container and various equipments, is summarized as follows:

(1) First, we must frame the yard map to indicate various avoidance distributions in yard. Therefore we use 2-dimensional lattices of a right-angle hexahedron in order to draw the yard map. Each lattice is used to specify proper addresses, i.e., the address (X_i, Y_i) is defined by the i-th address x_i on x-axis and the j-th address y_j on y-axis.

(2) To apply configuration space technique, which that the container is described as one point through the extension of container size for moving around a carrying container expressed in the yard map, we reframes the yard map into search space construction.

(3) We apply an optimal method for searching anti-collision path in yard space. In this paper, we select the optimal method for tracking the reference point based on experience information among available search methods.

To track the reference point effectively using Best-first search method (Sohn, 2003a), we first decide the evaluation function as follows:

$$F=\alpha_1 d_1+\alpha_2 d_2+\alpha_3 d_3 \tag{13}$$

where $\alpha_i (i=1, 2, 3)$ are weight values. In this paper, the coordinate point of container profile could be set as shown Table 1.

① d_1: It is defined by value that reflects the XY-plane upper from removable contiguity node t to goal node G.

$$d_1=\sqrt{(x_G-x_t)^2+(y_G-y_t)^2} \tag{14}$$

② d_2: It is defined by the orthogonal distance to line segment that connects the start node S and the goal node G in contiguity node t projected XY-plane upper to altitude as follows:

Table 1 The decision parameters of evaluation function

Notations	Descriptions
x_S, y_S	Start node coordinate value
x_G, y_G	Goal node of container coordinate value
x_n, y_n	Standard coordinate value of current node
x_t, y_t	Contiguity node from current node
x_p, y_p	Standard node value

$$d_2=\frac{|ax_t+by_t+c|}{\sqrt{a^2+b^2+c^2}} \tag{15}$$

Where the equation of straight line is given by

$$\begin{gathered} ax+by+c=0 \\ a=y_G-y_S,\ b=x_S-x_G \\ c=(x_G-x_S)\,y_S-(y_G-y_S)\,x_S \end{gathered} \tag{16}$$

③ d_3: The equation of straight line L_1 and L_2 is defined by

$$\begin{aligned} L_1&: \frac{x-x_p}{l_1}=\frac{y-y_p}{m_1}=\frac{z-z_p}{n_1}=t_1 \\ L_2&: \frac{x-x_p}{l_2}=\frac{y-y_p}{m_2}=\frac{z-z_p}{n_2}=t_2 \end{aligned} \tag{17}$$

where

$$\begin{gathered} l_1=x_n-x_p,\ l_1=x_t-x_n \\ m_1=y_n-y_p,\ m_2=y_t-y_n \\ n_1=z_n-z_p,\ n_2=z_t-z_n \end{gathered} \tag{18}$$

Then an angle d_3 is represented by

$$\cos d_3=\frac{l_1 l_2+m_1 m_2+n_1 n_2}{\sqrt{l_1^2+m_1^2+n_1^2}\sqrt{l_2^2+m_2^2+n_2^2}} \tag{19}$$

The anti-collision path is specified by the selection of weight values α_1, α_2, and α_3 used in Eq. (13), then we can search for the value of evaluation function that can be optimal path. The terms d_1, d_2, and d_3 in Eq. (13) are to guarantee approachability for searching the goal node, to be not escape from straight line between start point and goal point, and to select that the variant of direction angle of straight line to be connected by the created nodes, respectively.

4. Design of Neural Network Predictive PID Controller

4.1 2 DOF PID controller

In this paper, we will compose PID controller with 2 DOF that contains feedback type as shown in Fig. 5. This controller is very good effectiveness not only the estimation performance of fixing value but also the removal ability of disturbance. Therefore we study the problems to apply the position of an ATC and the anti-sway control of load.

First, the controller output $U(s)$ in Fig. 5 is described by:

$$U(s)=E(s)\left\{K_p(1-\alpha)+\frac{K_i}{s}+(1-\beta)K_d s\right\} - (\alpha K_p+\beta K_d s)\,Y(s) \quad (20)$$

where K_p, K_i, and K_d are gains of PID controller, respectively, the goal position and the swing angle of load is set by $Y(s)$, and the parameters α and β derive from the transformation of PID controller for various types. Moreover the necessary parameters for PID controller given by Eq. (20) is computed by NN auto tuning, and then the position error, length error of rope, and swing error are composed by the estimations of 15 parameters, respectively. The disturbance $D(s)$ is also considered by a strong wind of regular period at all times as follows:

$$F_\omega=p(3\sin\omega t+7\sin 2\omega t +5\sin 3\omega t+4\sin 4\omega t) \quad (21)$$

where ω is fundamental frequency of wind and p is wind magnitude.

4.2 Neural network modeling and predictive system

NNP system is composed of predictive system based on the present input/out information which is learned by executing the modeling learning about plant. The block diagram of neural network modeling learning and the proposed structure of 2-step NNP are shown in Figs. 6 and 7, respectively. In Fig. 7, the control parameter is the

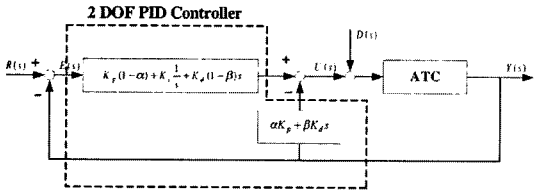

Fig. 5 PID controller with 2 DOF for an ATC

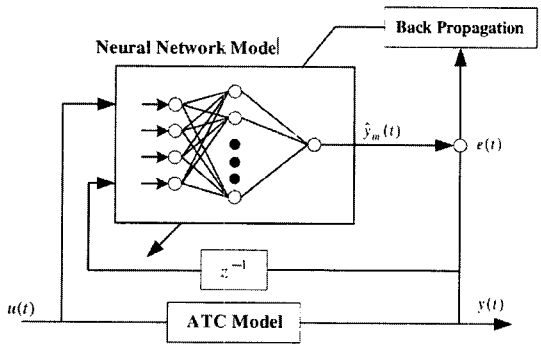

Fig. 6 Modeling of neural network

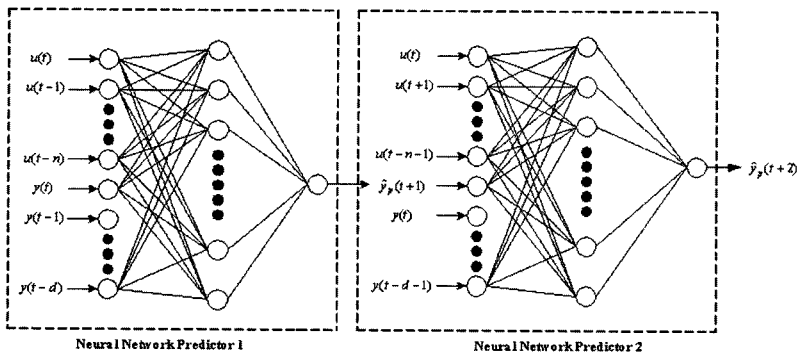

Fig. 7 Structure of neural network predictors

Table 2 The identification parameters for neural network modeling

		Parts of trolley position	Parts of swing angle
Pattern number		600	600
Node number	Input number	40	4
	Hidden number	6	6
	Output number	1	1
Learning ratio		0.09	0.09
Moment factor		0.03	0.03
Input parameters		$u(t)$, $u(t-1)$, $\hat{y}(t)$, $\hat{y}(t-1)$	$u(t)$, $u(t-1)$, $\hat{y}(t)$, $\hat{y}(t-1)$

position and angle of trolley. Also, the predictive output get using two NN predictors and the structure consists of 2-step predictor and the identification parameters for NN modeling is described by Table 2.

4.3 Neural network predictive PID controller

In this paper, we will propose the design results for PID controller to have ability to eliminate the disturbance and the performance to pursuer a target in order to control the stacking an ATC system. The proposed NNP PID control system is shown in Fig. 8. In this figure, the system configuration is composed of 3 parts ; i) Neural network predictor, ii) Neural network auto tuner, iii) PID controller. Neural network predictor can estimate the future output from the input information of current input/output of plant, and then NN auto tuner in order to compensate errors between the calculated predictive output and current output of plant computers parameters of controller through on-line learning scheme. Also, we used PID controller used to an industrial fields widely.

In general, PID controller is known that this controller to have a simple structure is easily realized by linear controller and should be ensure robustness certainly, however the actuate point of control system to require adaptiveness can not be sufficient control performances. To overcome this problem, we will compute parameters of PID controller using NN auto tuner and the structure of NN auto tuner is shown in Fig. 9. Here we

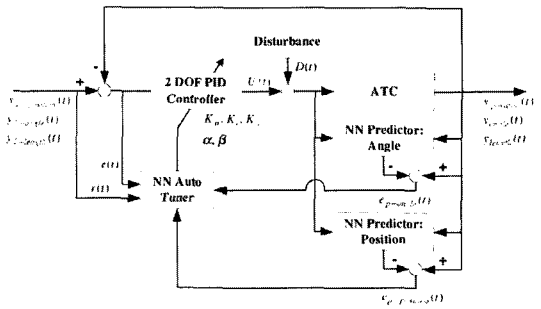

Fig. 8 A block diagram of neural network predictive PID controller

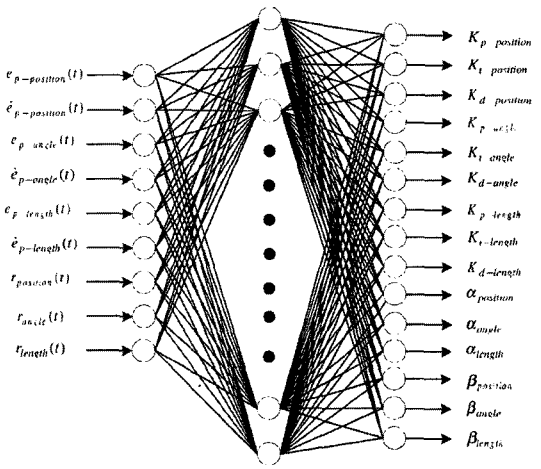

Fig. 9 Neural network auto tuner

use the momentum back propagation learning method and the input layer vector is composed of the error, the deviation of error, the predictive position of trolley, and an angle output and desired value. The activation functions of both

hidden and output layers are sigmoid and linear function, respectively. Learning rate and momentum constant of tuner is set to 0.9 and 0.5, respectively. Moreover all weights are set initially 0.5 to be chosen by trial and error.

In addition, we used NN algorithm to tune the parameters of PID control in online manners. The discrete time version of input of NNP PID controller is represented as follows:

$$\begin{aligned}u(t)=&\{(1-\alpha_p)k_{p\_p}(e(t)-e_p(t-1))+k_{i\_p}e_p(t)\\&+(1-\beta_p)k_{d\_p}(e_p(t)-2e_p(t-1)+e_p(t-2))\}\\&+\{(1-\alpha_a)k_{p\_a}(e(t)-e_a(t-))+k_{i\_a}e_a(t)\\&+(1-\beta_a)k_{d\_a}(e_a(t)-2e_a(t-1)+e_a(t-2))\}\\&+\{(1-\alpha_l)k_{p\_l}(e(t)-e_l(t-1))+k_{i\_l}e_l(t)\\&+(1-\beta_l)k_{d\_l}(e_l(t)-2e_l(t-1)+e_l(t-2))\}\\&-\{\alpha_p k_{p\_p}(y_p(t)-y_p(t-1))\\&+\beta_p k_{d\_p}(y_p(t)-2y_p(t-1)+y_p(t-2))\}\\&-\{\alpha_a k_{p\_a}(y_a(t)-y_a(t-1))\\&+\beta_a k_{d\_a}(y_a(t)-2y_a(t-1)+y_a(t-2))\}\\&-\{\alpha_l k_{p\_l}(y_l(t)-y_l(t-1))\\&+\beta_l k_{d\_l}(y_l(t)-2y_l(t-1)+y_l(t-2))\}\end{aligned} \tag{22}$$

where $e=[e_p(t)\ \ e_a(t)\ \ e_l(t)]^T$ and the parameters given by Eq. (22) are shortly described as the subscripts of parameters shown in Fig. 9. For simplicity, note that $e_{p-position}(t)$, $e_{p-angle}(t)$ and $e_{p-length}(t)$ are expressed by $e_p(t)$, $e_a(t)$ and $e_l(t)$, respectively.

Also, the disturbance is used in Eq. (21) and the estimation function is used error function using the following equations

$$\begin{aligned}E&=\frac{1}{2}[y_{d-position}(t)-x(t)]^2\\E&=\frac{1}{2}[\theta_{d-angle}(t)-\theta(t)]^2\\E&=\frac{1}{2}[y_{d-length}(t)-l(t)]^2\end{aligned} \tag{23}$$

Error function E in Eq. (23) can be minimized by adjusting weight values. Note that it finds minimum of error function by the gradient descent. Based on the gradient descent method, both output layer and hidden layer are described by:

$$\begin{aligned}\Delta W_{jk}(t)&=-\eta\frac{\partial E}{\partial W_{jk}}+E\Delta W_{jk}(t-1)\\\Delta W_{ij}(t)&-\eta\frac{E\partial}{\partial W_{ij}}+\varepsilon\Delta W_{ij}(t-1)\end{aligned} \tag{24}$$

where η and ε are the learning rate and momentum constant, respectively. Then the error signal of output layer is given by (Choi, 2001)

$$\begin{aligned}\delta_k&=-\frac{\partial E}{\partial net_k}\\&=-\frac{\partial E}{\partial y(t+1)}\frac{\partial y(t+1)}{\partial u(t)}\frac{\partial u(t)}{O(k)}\frac{\partial O(k)}{\partial net_k}\end{aligned} \tag{25}$$

where

$$net_k=\sum_j W_j kO_j+\theta_k \tag{26}$$

$$o_{pj}(k)=f_j(net_{pj})=f_j(\sum_j w_{ji}o_j) \tag{27}$$

Then, using the chain rule, the update weights between hidden layer and output layer is calculated by:

$$\Delta W_{jk}(t+1)=\eta\delta_k O_j+\varepsilon\Delta W_{jk}(t) \tag{28}$$

Note that the error signals of each node for output layer, the Jacobian of system, and the derivative equation of output layer for each NN node are described by our previous researches, respectively (Werbos, 1992).

5. Numerical Simulations

To evaluate the NNP PID controller proposed in this paper, we execute numerical simulation about an ATC model and describe the relative analysis for the position of container, sway control, and the load variation for disturbance and container using PID controller and NNP PID controller. The considered ATC system is shown

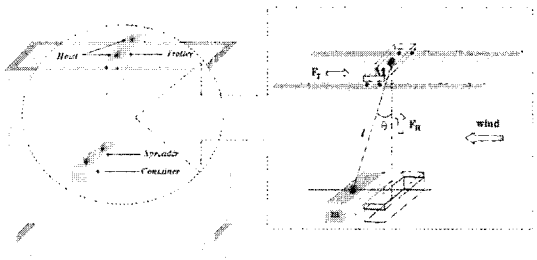

Fig. 10 The structure of an ATC system

in Fig. 10 and the numerical parameters for computer simulation are shown in Table 3. The NN modeling for composing the proposed NNP PID controller is each 3rd floor structure and each node of input layer, hidden layer, and output layer for NNP PID controller is 4, 6, and 1, and each node of auto-tuner of NN is also 9, 21, and 15, respectively.

Table 3 Numerical parameters for an ATC

Parameters	Values
Gravity acceleration	9.8 [m/s^2]
Trolley load	4.2 [kg]
Container load	10 [kg]

In Fig. 11, we describe the response characteristics for PID and NNP PID controllers when the weight of container for an ATC is 10 [kg]. Then the main characteristics of each item for PID and NNP PID controllers are compared with Table 4, respectively.

Moreover, in order to evaluate robustness and stability of an ATC system, we analyze the response characteristics of PID and NNP PID controllers as shown in Fig. 12. In this figure, the weight of container increases about 15 [kg] and the disturbance is added by an initial state of disturbance. In these cases, the main characteristics of each item for PID and NNP PID controllers are compared with Table 5, respectively.

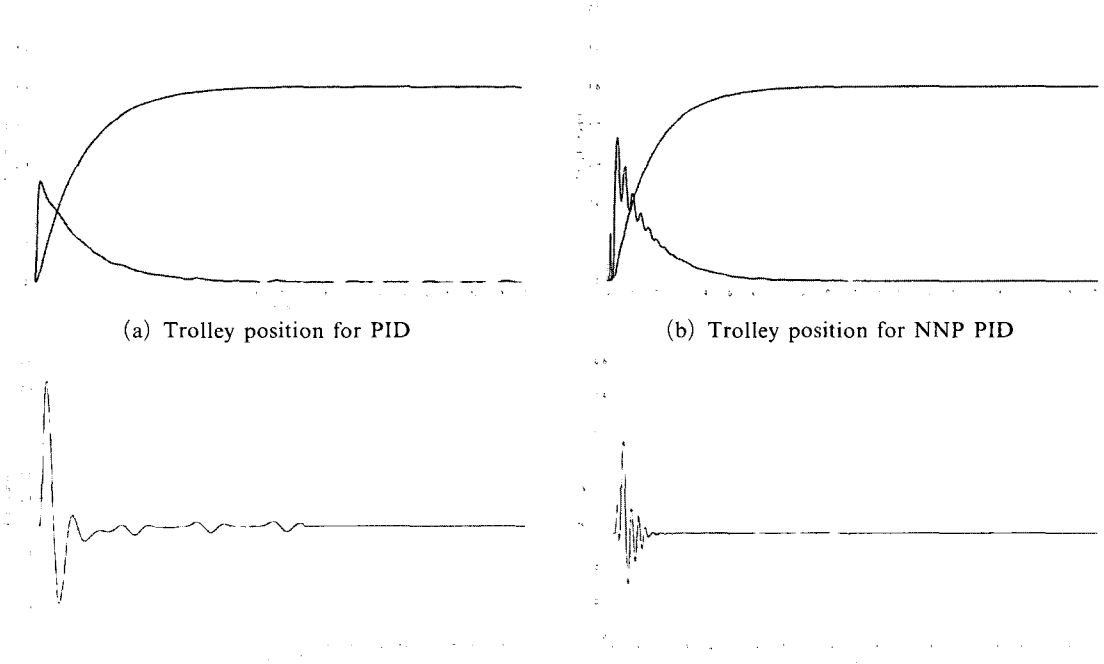

(a) Trolley position for PID

(b) Trolley position for NNP PID

(c) Angle for PID

(d) Angle for NNP PID

Fig. 11 Rsponse characteristics of PID and NNP PID

Table 4 Comparison of PID and NNP PID controllers for an ATC

Response characteristics		PID controller	NNP PID controller
Position control	Position settling time [sec]	9.75	11.25
Swing control	Swing angle [degree]	−0.2745~0.5244	−0.1455~0.2677
	Swing settling time [sec]	14.25	11.25

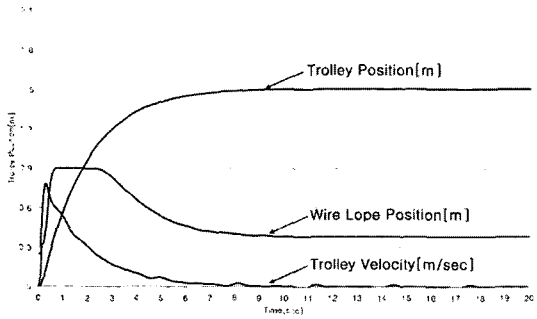

(a) Trolley position for PID

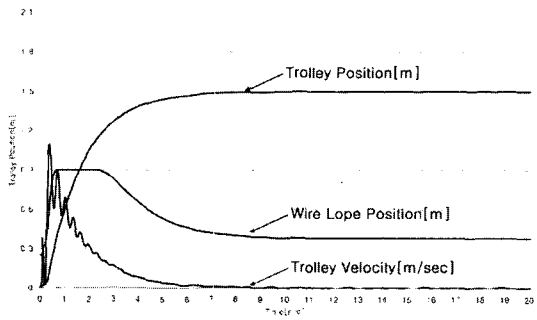

(b) Trolley position for NNP PID

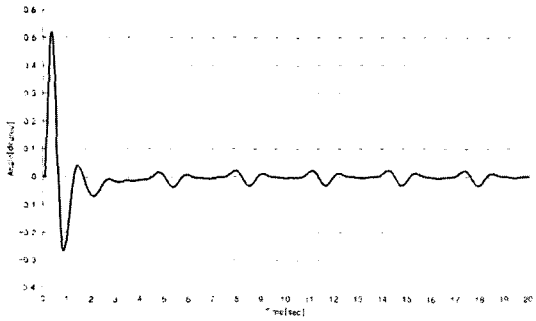

(c) Angle for PID

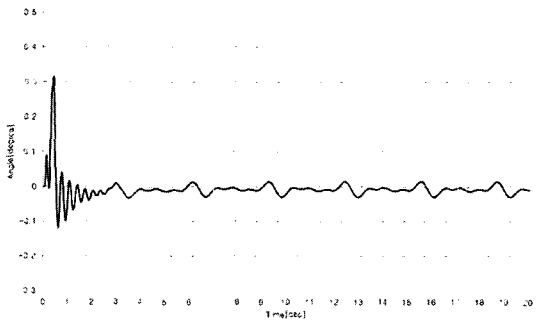

(d) Angle for NNP PID

Fig. 12 Response characteristics of PID and NNP PID for disturbance (a wind force)

Table 5 Comparison of PID and NNP PID controllers for an ATC about disturbance

Response characteristics		PID	NNP PID
Position control	Position settling time [sec]	10.9	10.75
	Position error [m]	0.001936~0.007801	−0.000638~0.002043
Swing control	Swing angle [degree]	−0.2675~0.51804	−0.1186~0.31293
	Amplitude of swing angle [degree]	−0.02856~0.01988	−0.02817~0.01163

6. Experimental Results

6.1 System configuration of an ATC

The structure of an ATC simulator manufactured in this paper is shown in Fig. 13. The magnitude of an ATC simulator and the volume of a container are $W3580 \times D540$ mm $\times H1640$ mm and $W600 \times D240 \times H130$ mm, respectively.

Moreover the schematic diagram for experiment is also shown in Fig. 14 and the manufactured ATC system is composed of four parts; i) control part, ii) driving part, iii) communication part, and iv) sensor part. In this system, since the information of driving error is transmitted to *DSP* through *RS232* communication, it can be exchanged with the information for driving controller and composed of generating the driving signals of each motor by receiving encoder datum such as control algorithm in DSP, the

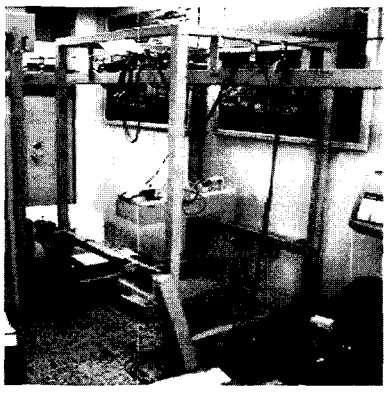

Fig. 13 Structure of an ATC simulator system

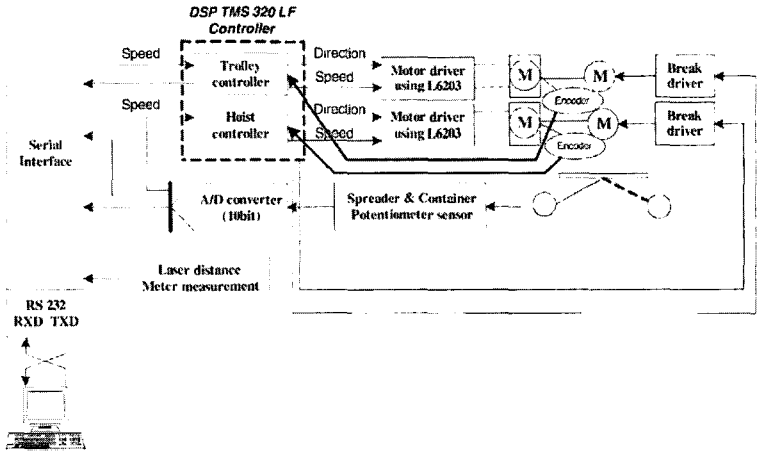

Fig. 14 Schematic diagram of an ATC System

distance and position between trolley and hoist of an ATC system, etc.

As we observe the motion process of automatic driving control for an ATC system shown in Fig. 14, we estimate an anti-sway angle and position using potentiometer and encoder, respectively. Furthermore we can compute a control input form the estimate value to be inputted from PC, and then the velocity command of motor is given by the control input calculated through DSP.

6.2 Learning and test of NN model for an ATC system

NN tuner shown in Fig. 9 is tuned by eq. (28) on the one step and by online. However the tuner was tuned enough to satisfy the following condition without the actual plant by using NN models in order to avoid an initial damage at the tuner applying. The parameters of NN tuner such as weights were memorized whenever simulations and experiments were performed. Then the parameters of NN tuner are also specified as follows :

① Learning Rate : 0.9
② Momentum Rate : 0.5
③ No. Inputs : 15
④ Hidden Layer Size : 38
⑤ No. Outputs : 15

In an initial tuning work without plant, the parameters of NN models that are used identifiers

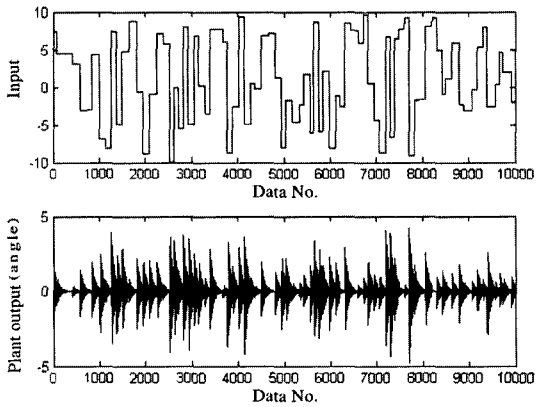

Fig. 15 Training data for NN angle model

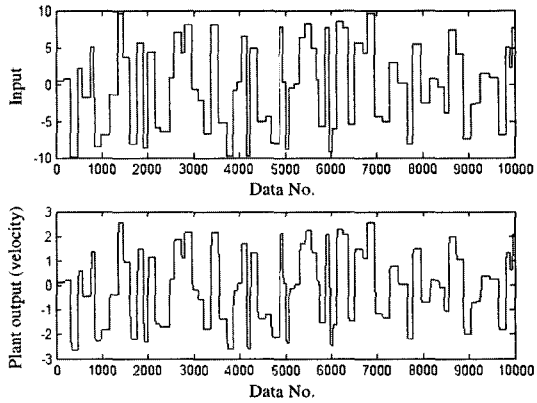

Fig. 16 Training data for NN position model

and system predictor for the sway and trolley driving are given by

① No. Delayed Plant Inputs : 3

② No. Delayed Plant Outputs : 8
③ Hidden Layer Size : 38
④ Training samples : 10000
⑤ Epochs : 50

NN learning samples and its results of identification of angle and position model are shown as Figs. 15 and 16, respectively. In the case of NN model for the position of trolley used the learning, the learning is not performed well. Therefore the position of NN model is learned by trolley speed with integrator. Furthermore the test results for both of NN models are shown as Figs. 17 and 18, respectively. Errors between the model and plant are less than 10^{-6}.

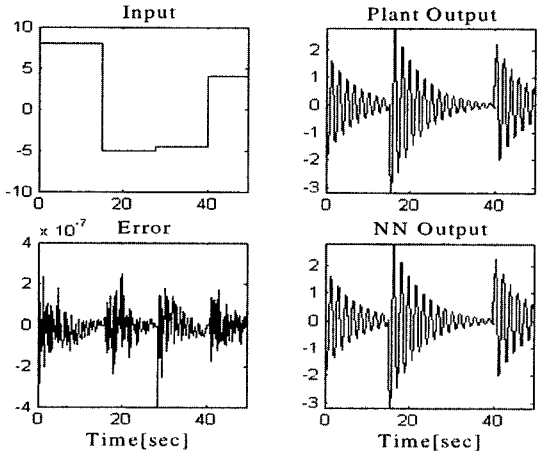

Fig. 17 Test result of NN angle model

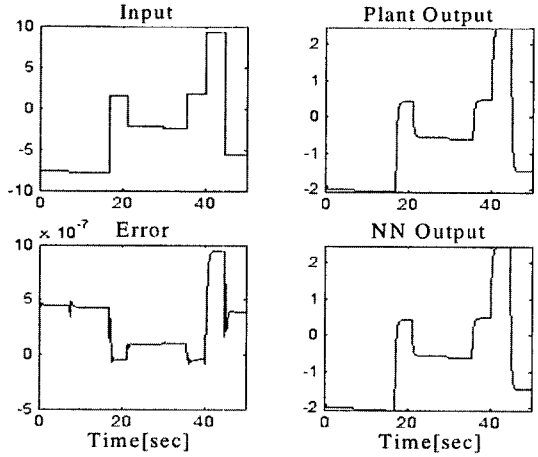

Fig. 18 Test result of NN speed model before its integrated distance model

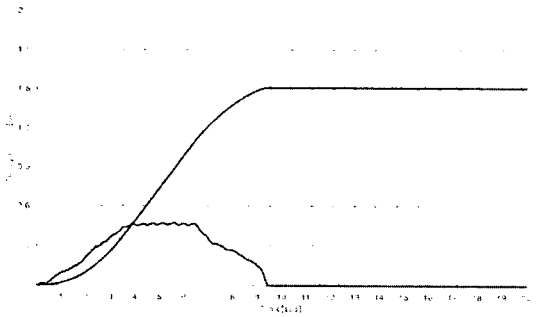

(a) Trolley position for PID

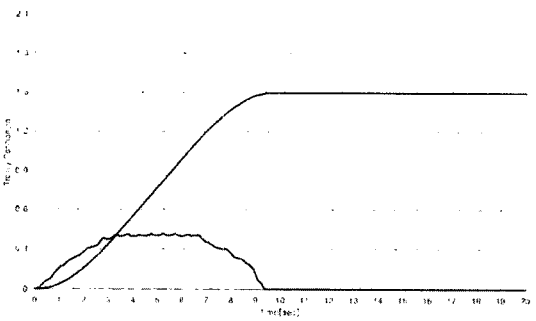

(b) Trolley position for NNP PID

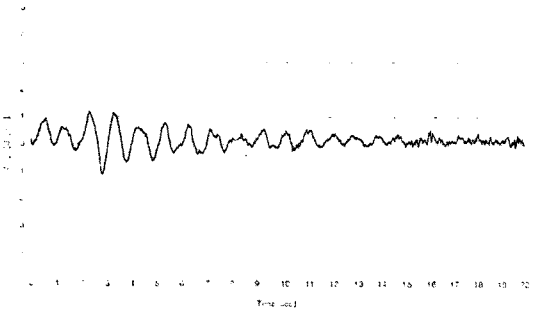

(c) Angle for PID

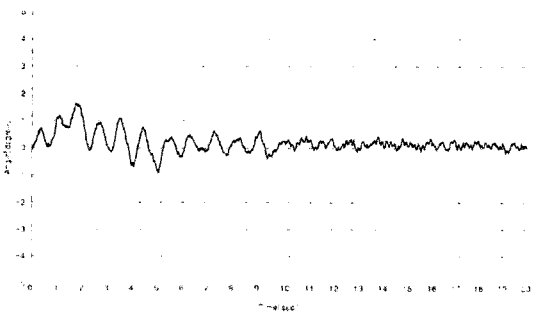

(d) Angle for NNP PID

Fig. 19 Experimental results with response characteristics of PID and NNP PID

6.3 The realizations of PID and NNP PID controllers for an ATC system

Figure 19 shows the experimental results with response characteristics of PID and NNP PID controllers when the weight of container for an ATC is 10 [kg]. Here, when the final target position and the initial angle of an ATC set up 1.5 [m] and 0 [degree], respectively, we experiment on the estimate state to the target position 1.5 [m] of trolley. Moreover the main characteristics of each item for PID and NNP PID controllers are compared with Table 6, respectively.

Furthermore we show the response characteristics of PID and NNP PID controllers as

Table 6 Comparison of PID and NNP PID controllers for an ATC

Response characteristics		PID	NNP PID
Position control	Position settling time [sec]	9.4	9.4
	Position error [m]	0.0077	−0.0032
Swing control	Swing angle [degree]	−1.0845~1.1655	−0.8464~1.6284
	Amplitude of swing angle [degree]	−0.0675~0.4905	−0.046~0.4142

Table 7 Comparison of PID and NNP PID controllers for an ATC about disturbance

Response characteristics		PID	NNP PID
Position control	Position settling time [sec]	14.95	14.20
	Position error [m]	0.005785	0.004992
Swing control	Swing angle [degree]	−1.6704~1.7302	−1.4896~1.7248
	Amplitude of swing angle [degree]	−0.3376~0.2994	−0.3430~0.2450

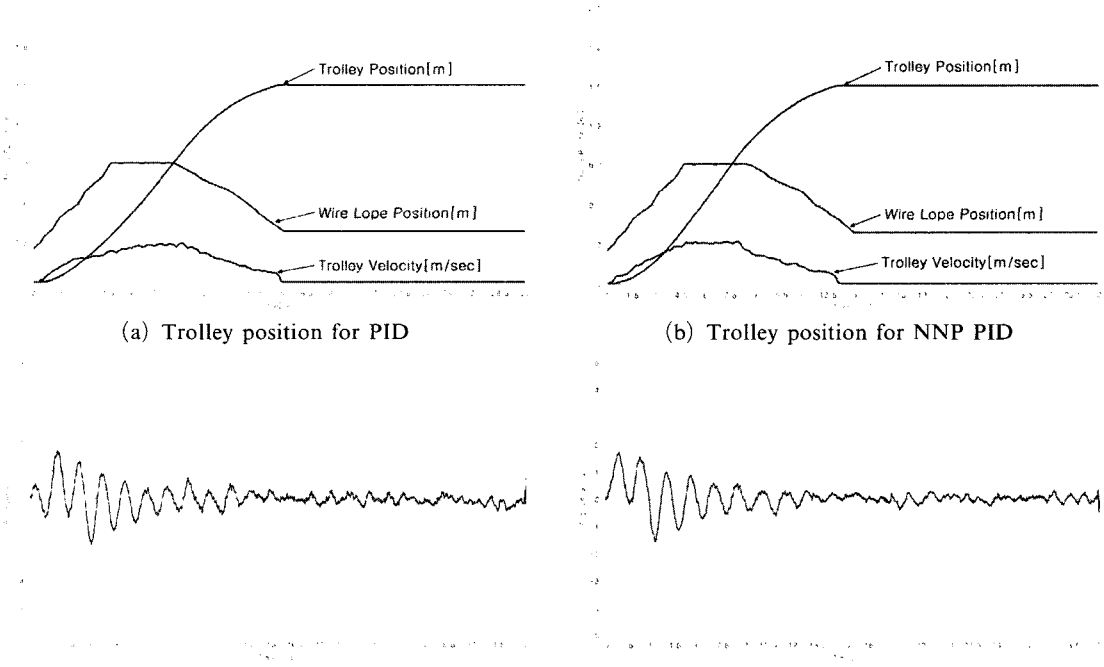

(a) Trolley position for PID

(b) Trolley position for NNP PID

(c) Angle for PID

(d) Angle for NNP PID

Fig. 20 Experimental results with response characteristics of PID and NNP PID for disturbance (a wind force)

shown in Fig. 20. In this figure, the weight of container increases about 15 [kg] and the disturbance is also added by an initial state of disturbance. Moreover the main characteristics of each item for PID and NNP PID controllers with a wind force are compared with Table 7, respectively. Compared with each term, we know that swing angle of NNP PID controller decreases more 0.1862 [degree] than PID controller and the amplitude of swing angle also decreases more 0.049 [degree] than PID controller.

7. Conclusions

In this paper, we develop anti-sway control in proposed techniques for an ATC system. First, the developed algorithm is to build the optimal path of container motion and to calculate an anti-collision path for collision avoidance in its movement to the finial coordinate.

In order to show the effectiveness in this research, we compared NNP PID controller to be tuning parameters of controller using NN with 2 DOF PID controller. The simulation and experimental results show that the proposed control scheme guarantees good performances, trolley position, sway angle, and settling time in NNP PID controller than other controller. By using the proposed controller, there were improvements of 4.7% and 13.6% for settling time and trolley position error than the conventional PID controller respectively. Moreover, the sway angle could be reduced to 5.5% by NNP PID controller. We researched about develop of the ATCS in the techniques for unmanned automation of the ATC. Besides, we designed the NNP PID controller using the NN predictor, and compared with the conventional controller. As result, the application of NNP PID controller is analyzed to have robustness about disturbance which is wind of fixed pattern in the yard. Accordingly, the proposed algorithm proposed in this study can be readily used for industrial applications.

Acknowledgment

The work was supported by the National Research Laboratory Program of the Korean Ministry of Science and Technology (MOST).

References

Canbulut, F., Sinanoglu, C. and Yildirim, S., 2004, "Analysis of Effects of Sizes of Orifice and Pockets on the Rigidity of Hydrostatic Bearing using Neural Network Predictor System," *KSME International Journal*, Vol. 18, No. 3, pp. 432~442.

Choi, S. W., 2001, "A Development of ATCS for Automatic Transfer Crane," M. D. Thesis, Dong-A University, Busan, Korea.

Furuta, K., 1980, State Variable Methods in Automatic Control, John Willey and Sons.

Kim, Y. B., 2004, "A New Approach to Anti-Sway System Design Problem," *KSME International Journal*, Vol. 18, No. 8, pp. 1306~1311.

Klaassens, J. B., Honderd, G., Azzouzi, A. E., Cheok, K. C. and Smid, G. E., 1998, "3D Modeling Visualisation for Studying Controls of the Jumbo Container Crane," *Proc. of the American Control Conference*, pp. 1754~1758.

Kwok, K. S. and Drissen, B. J., 1999, "Path Planning for Complex Terrain Navigation via Dynamic Programming," *Proc. of the American Control Conference*, pp. 2941~2944.

Lee, H. H., 1997, "Modeling and Control of a 2-Dimensional Overhead Crane," *Proc. of the ASME Dynamic Systems and Control Division*, Vol. 61, pp. 535~542.

Lee, H. H., 1998, "Modeling and Control of a Three-Dimensional Overhead Crane," *ASME Journal of Dynamic Systems, Measurement, and Control*, Vol. 120, No. 4, pp. 471~476.

Lee, J. K., Park, Y. J. and Lee, S. R., 1996, "Development of a Motion Control Algorithm for the Automatic Operation System of Overhead Crane," *Trans. on KSME in Korea*, Vol. 20, No. 10, pp. 3160~3172.

Sakawa, Y. and Shindo, Y., 1982, "Optimal Control Container Crane," *Trans. on IFAC*, Vol. 18, No. 3, pp. 257~266.

Sohn, D. S., Min, J. T., Lee, J. W., Lee, J. M. and Lee, K. S., 2003, "A Study on Development of ATCS for Automated Transfer Crane using

Neural Network Predictive PID Controller," *Proc. of SICE Annual Conference*, pp. 3170~3175.

Suh, J. H., Lee, Y. J. and Lee, K. S., 2004, "Anti-sway Control of an ATC using NN Predictive PID Control," *Proc. of the 30th Annual Conference on the IEEE Industrial Electronics Society*.

Werbos, P. J., 1992, "Neural Networks and Human Mind ; New mathematics fits humanistics insight," *Trans. on IEEE Systems, Man, and Cybernetics*, Vol. 1, pp. 78~83.